ASIA TURBOMACHINERY & PUMP SYMPOSIUM
13-15 MARCH 2018 | SINGAPORE

TUTORIAL: ROTOR-BEARING DYNAMICS OF INTEGRALLY GEARED TURBOMACHINERY

Karl Wygant
Vice President
Hanwha Power Systems
Houston, TX, USA

Dr. Wygant is a Vice President at Hanwha Power Systems and is currently located in Houston, TX. Dr. Wygant holds an M.S. and Ph.D. in Mechanical Engineering from the University of Virginia and an M.B.A. from Norwich University. His engineering experience over the last 25 years is related to a wide variety of turbomachinery including: rocket turbopumps, automotive turbochargers, industrial compressors, steam turbines, gas turbines, and novel turbomachinery applications. His management background includes: project management, multi-group management, business management, and leading new product development from inception to market delivery.

Chad Robertson
Senior Engineer
Hanwha Power Systems
Houston, TX, USA

Mr. Robertson is a Senior Engineer at Hanwha Power Systems and is currently located in Houston, TX. Mr. Robertson holds a B.S. in Mechanical Engineering from Texas A&M University. He has 12 years of experience in gear design and manufacturing and has worked on a wide variety of gearing applications spanning form high speed turbomachinery to low speed mill drives. Prior to joining Hanwha worked for Lufkin Industries part of GE Oil and Gas. Mr. Robertson has previously served as a member on the Sound and Vibration Committee for the American Gear Manufacturers Association, AGMA.

Fang Li
Senior Engineer
Hanwha Power Systems
Houston, TX, USA

Dr. Li is a Senior Engineer at Hanwha Power Systems and is currently located in Houston, TX. Dr. Li holds a Ph.D. in Mechanical Engineering from the Georgia Institute of Technology, an M.S. from Chinese Academy of Science and a B.S. from Tsing Hua University at Beijing, China. His engineering background includes solid, fracture, thermal mechanics, structural and dynamics analysis. He has worked in a variety of industry includes aircraft, green energy and turbomachinery.

ABSTRACT

This tutorial focuses on the rotordynamic characteristics of integrally geared compressors and expanders. Although the focus is for turbomachinery the topics discussed also apply to industrial gearing. The topics covered include understanding the influence of gear forces, thrust collars (hydrodynamic elements that transmit load from pinion shaft to bull gear shaft), and thrust bearings on the reaction loads of the pinion and bull gear bearings. The various aspects that couple the pinion and bull gear dynamics such as: 1) gear contact stiffness and 2) thrust collar moment stiffness are examined to show the influence of coupled pinion-bull gear rotordynamics. Torsional, lateral, and axial rotordynamic behavior of geared systems is discussed relative to different design standards: API617, API672, etc. Various case studies are presented that show the vibration characteristics for common field and shop problems. The case studies used to illustrate the topics presented show the origin of "step increases in vibration," "sub-synchronous vibration originating from aerodynamic excitation and bull gear harmonics on the pinion shafting.

INTRODUCTION

Background

An integrally geared compressor, IGC, is comprised of one or more compressor stages attached to the end of one or more high speed pinions. The pinions are mounted in a housing that contains a large low speed bull gear which drives the individual pinions. Figure 1 shows an exploded view of a typical IGC.

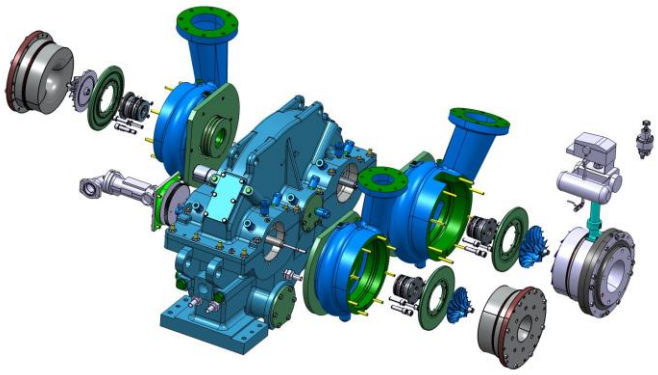

Figure 1. Exploded View of Integrally Geared Compressor

One of the advantages of an integrally geared compressor is that intercooling can be, and most often is, applied between stages to reduce the aerodynamic power consumed. Figure 2 shows a configuration of a multi-stage integrally geared compressor that

applies intercooling between the stages.

Figure 2. Integrally Geared Fuel Gas Compressor Sitting Atop Three Inter-Coolers with Motor in Background.

Relevant Literature

There are a number of relevant articles related to the design of integrally geared turbomachines. Fingerhut, et. al [1991] observes that since the 1950's, integrally geared centrifugal compressors have been in use worldwide, initially in plant air applications, and increasingly in the process industry.

The integrally geared centrifugal compressor has successfully been utilized in a large range of applications in the process industry starting with compressors operated purely on air, followed by nitrogen. Now applications can be found with carbon monoxide, carbon dioxide, chlorine, hydrocarbons, acetylene, isobutyric aldehyde, and various other process gasses.

Beaty, et. al. [2000] describes the advantages and risks associated with an integrally geared compressor. In the author's assessment aspects such as: capital cost, installation cost, operating cost, durability, downtime, and maintenance costs are all assessed. The authors list the reduced capital, installation, and operating costs resulting from a compact IGC and the ability of the IGC to have individual pinion rotating speeds to maximize stage efficiency. Wehrman, et. al. [2003] reported that the direction of the industrial gas business was such that complex integrally geared compressors were starting to be required. The authors presented a tutorial to give examples on design issues and experiences from two companies that operate and use IGCs. Srinivasan [2013] describes the evolution of IGCs entering the process gas industry with several relevant examples. The author describes how multiple rotor speeds from the individual pinions are applied to achieve an aerodynamically efficient design for each stage. Wygant [2016] describes the various applications for integrally geared compressors and lists the many challenges in designing for each application.

Substantial work has been published in the past several years regarding both the prediction and measurement of vibration in integrally geared turbomachines.

Williams [2015] defines several causes of sub-synchronous vibration, SSV, that are common to integrally geared compressors. The author states that the pinion shafts in integrally geared compressors tend to create a vibration response that is quite different from inline compressors. The authors review vibration monitoring techniques with a focus on how they can be applied to identify common symptoms of vibrations. A systematic approach is essential to resolving sub-synchronous vibration problems in IGC's. The challenge being that a single root cause may not be the culprit, or origin, of the issue.

Zhang, et. al., [2016] investigates the dynamic behaviors of the geared turbomachinery systems with changes to in workload. (The variations in workloads can result from changes in flow conditions as a result of inlet guide vane settings.) The analytics examines the impact of bearing dynamic coefficients, axial force and torque, and varying levels of gear mesh stiffness on the dynamics. The results show that even though the rotors of the geared system do not have critical speeds close to the rated speeds, that changes in the load on the compressor can shift resonance conditions.

Smith [2011] describes a case where the high-speed pinion had a damped natural frequency very close to the operating speed of the low speed pinion that was transmitted through the bull gear and excited the damped natural frequency causing SSV which lead to bearing wear. It was discovered that excessive pitch line and thrust collar runout on the low speed pinion contributed to transmitting the vibration energy across the bull gear to the other pinion. This is a good example of how the vibration of one pinion can act as a source of vibration on a separate pinion. The lateral transmissibility of a gear train is dependent on the design of the pinion and bullgear geometry, gear teeth geometry, support stiffness and damping provided by the bearings. Based on that author's experience, synchronous lateral vibration of one pinion is more likely to transmit through the bullgear to the accompanying pinion than an SSV of equal or greater amplitude.

The ability to determine between normal operational vibration characteristics and problematic vibrations can be found roughly through API 672 guidelines. Srinivasan [2012] goes further and highlights that there are cases where sub-synchronous vibrations are benign and there are cases where concern should be present. The ability to distinguish between those two scenarios requires extensive knowledge of integrally geared turbomachinery operation.

Objective

The objective of this tutorial is to describe the various factors that influence the vibration of integrally geared turbomachines. This includes susceptibility to instabilities, unbalance response, and vibration transmission from other sources. Analytics are presented that show the impact of

coupling through gear mesh stiffness and/or moment stiffness of thrust collars. And the tutorial ends with several relevant small case studies to show field and test stand implications of the topics addressed herein.

STATIC AND TRANSIENT FORCES

Commonly Used Gear Types in Integrally Geared Turbomachinery

Most industrial integrally geared turbomachines are single helical gears. Double helical gears are typically not utilized with IG machines for several reasons. External aerodynamic thrusts can cause uneven loading on the opposing helices. Additionally with double helical gearing the pinion typically is allowed to float axially with no thrust bearing. The gear forces act to center and locate the pinion during operation, but the backlash of the teeth and the thrust bearing of the bull gear are what mechanically limits the axial movement. The amount of axial movement on a double helical pinion is typically large enough that if sufficient clearance was designed into the impeller and volute to avoid potential impact the aerodynamic efficiently is greatly reduced compared to what can be accomplished with single helical gearing.. Spur gears are not typically used for industrial turbomachinery because the helical gears provide quieter operation and the larger torque transfer capability. Figure 3 shows both a single helical gear and a double helical gear turbomachine.

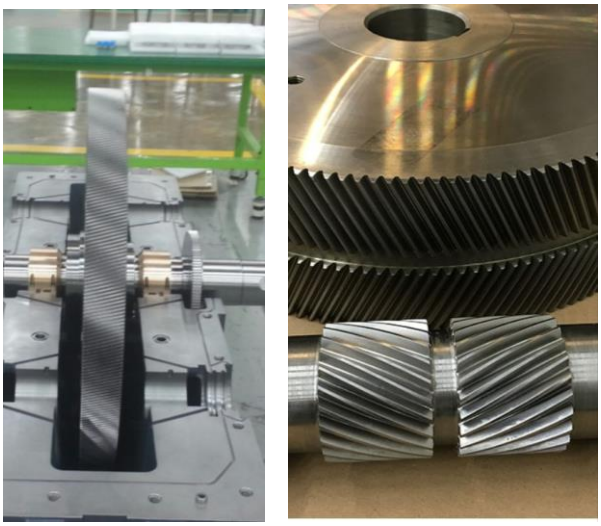

Single Helical Gear *Double Helical Gear*

Figure 3. Single and Double Helical Gear Systems

Systems with Thrust Bearings and Thrust Collars

Thrust bearings on the pinion shaft transmit the net axial load from the aerodynamics and gear axial force through the thrust bearing to the static bearing housing. Thrust collars transmit the net axial force from the aerodynamics and the gear mesh to the bull gear disk axial surface. The net residual thrust is then resolved against the bull gear thrust bearing (a lower speed and lower loss mechanism.) Thrust bearings provide greater levels of thrust capacity whereas thrust collars have significantly reduced parasitic losses. Figure 4 shows a pinion with thrust collars. Figure 5 shows a pinion shaft and combination journal/thrust bearings.

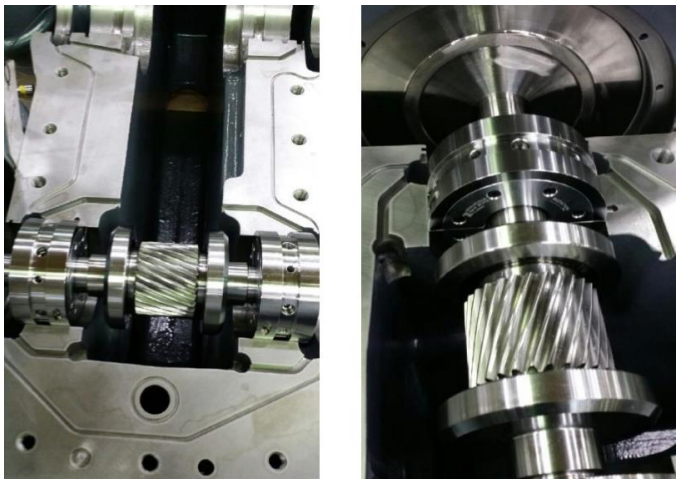

Figure 4. Example of pinion gear-shaft with thrust collars on either side.

Figure 5. Example of pinion gear-shaft with thrust bearings on either side.

Free Body Diagrams

Of course the journal bearings must react the gravity and gear radial and tangential forces. But a clear understanding of the axial forces is also critical to understanding the bearing loads. A clear understanding of the resolution of forces for the axial loads is essential to understanding the net loading on the radial bearings. The reason for this is that the line-of-action for thrust collars and thrust bearings does not correspond with both the gear mesh and aerodynamic axial forces. Therefore a moment is created that must be resolved by the radial bearings. Failure to account for this moment means that the incorrect loading is

defined on the bearings and not only the thermal characteristics may be different between measurement and prediction, but the resulting rotordynamic performance can vary as well. Consider three cases: a double helical gear with no thrust control, a single helical gear with thrust bearing and a single helical gear with thrust collars. Figure 6 shows the free-body diagram of a double helical gear system. Note that double helical gear systems are not frequently used with integrally geared turbomachines. The reason for this becomes evident as the axial load transmission from the aerodynamics must be resolved with the mesh system. As a result one helical gear surface is more highly loaded than the other.

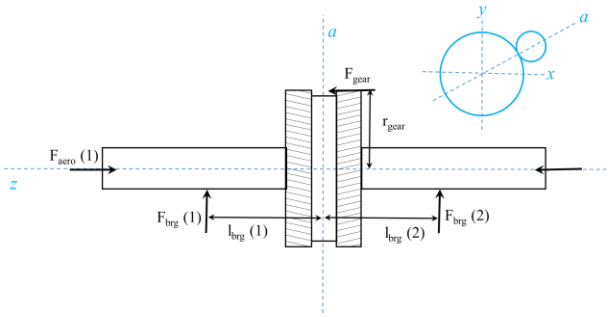

Figure 6. Free Body Diagram of Double Helical Gear System

Single helical gears are the most common gear system in IG turbomachinery. The single gear is less material than the double, able to resolve thrust outside the gear system, and preferable in terms of rotordynamics and cost. Figure 7 shows the free body diagram for a single helical gear system with thrust bearing. Notice that the line of center for the thrust bearing reaction force is not the same as that of the gear mesh axial force. Therefore the gear mesh acts to create a moment that must be resolved by the radial bearings. That moment tends to create reactions in the radial bearings that are in opposite radial directions.

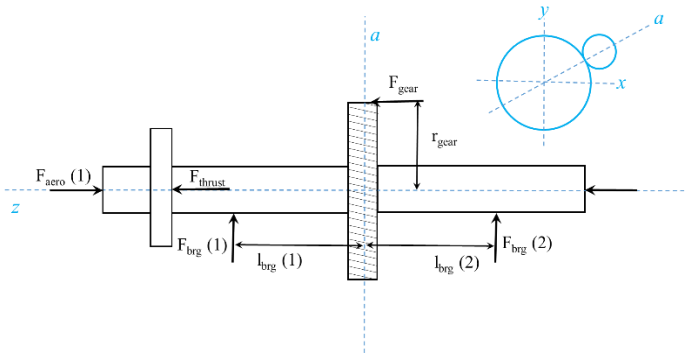

Figure 7. Free Body Diagram of Single Helical Gear Pinion with Thrust Bearings

To minimize the parasitic losses and also reduce the amount of lubricant, the vast majority of air compressors apply thrust collars to manage the thrust on the pinion. Figure 8 shows the free body diagram of a pinion shaft that uses thrust collars to transmit the thrust to the bull gear shaft.

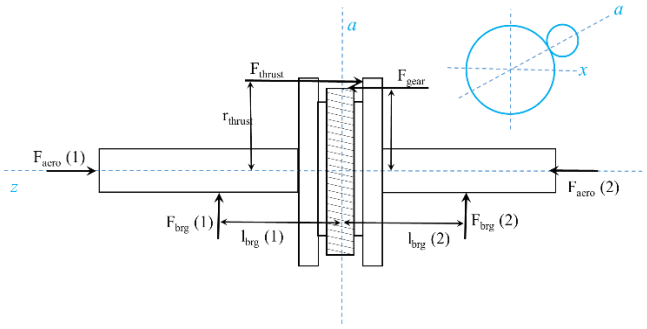

Figure 8. Free Body Diagram of Single Helical Gear Pinion with Thrust Collars

Static Equilibrium

To determine the static load on the bearings the gravity force, radial, and axial forces of the gear must be known. Also the aerodynamic pressures must be integrated and resolved into a net axial force and the type thrust control mechanism must be correctly applied. Equations 1 through 3 may be used to resolve the net radial load from the gears on to the bearings.

$$\sum F_{axial} = 0 \quad (1)$$

$$\sum F_{radial} = 0 \quad (2)$$

$$\sum M_{a-z} = 0 \quad (3)$$

By solving the resulting radial and axial forces and the moments, the radial loads on the bearing can be determined. Based on the type of gear and the thrust management system the radial loads will vary.

Transient Loading as a Function of Steady State Loading

To correctly resolve the radial loads on the journal bearings of the pinions requires: gravity load, gear radial loads, and moment reactionary loads from the axial forces. Further complicating matters is that these loads all vary with the aerodynamic conditions and torque transmission through the system. Figure 9 shows the gravity and gear forces acting on the journal bearings of the pinion. Figure 10 shows the resulting shaft orientation resulting from gear and gravity loads acting on a journal. Notice that the pinion bearing load direction is strongly dominated by the gear radial load. The end result is that the rotordynamics and bearing performance of integrally geared turbomachines must be tolerant to loading at a variety of attitude angles. On a tilting pad journal bearing the loading can be on-pad, off-pad, or somewhere in-between.

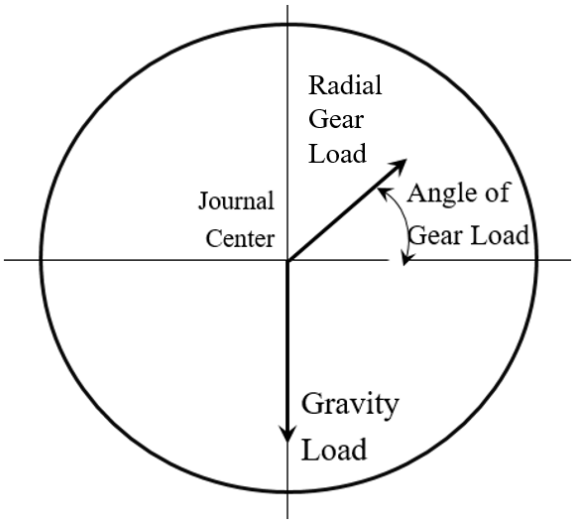

Figure 9. Influence of gravity and gear forces acting on bearings.

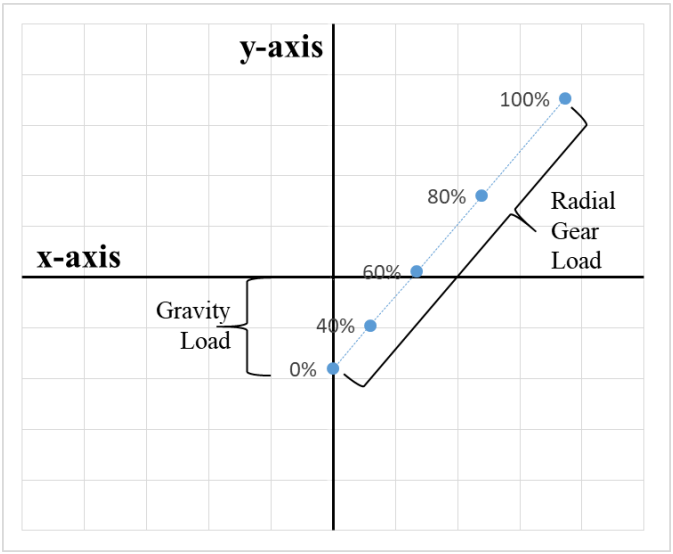

Figure 10. Magnitude and phase as a function of gear load

BULLGEAR AND PINION CONNECTIVITY

The gear mesh adds significant stiffness near the center of the rotor and can affect the dynamic characteristics. Gear mesh stiffness is a complex phenomenon, but API 684 Section 2.8.3 provides equations to estimate the stiffness coefficients in meshing gears. The equations are as follows.

$$K' = C(FW)cos^2(\beta)10^6 \quad (4)$$
$$K_{xx} = K'cos^2(\gamma) \quad (5)$$
$$K_{xy} = K'sin(\gamma)cos(\gamma) \quad (6)$$
$$K_{xy} = K_{yx} \quad (7)$$
$$K_{yy} = K'sin^2(\gamma) \quad (8)$$

The author has contacted several of the API committee members to determine the origins of this equation and found that the equations were provided by a gear manufacturing company but other details about the origins are unknown. It is suspected that formulas are derived from empirical data from tests on spur gears and adjusted for helical gearing. The following section attempts to derive the provided equations for future reference.

Buckingham [1949] derived the following formulas for deflection of spur gear teeth based on experimental work of the ASME Research Committee and Wilfred Lewis in 1931. Equation 9 gives deflection values from combined tooth bending and Hertzian compression of the mating gear teeth for a 20 degree normal pressure angle full tooth form.

$$d = \frac{9.000\,W}{F}\left(\frac{1}{E_1} + \frac{1}{E_2}\right) \quad (9)$$

Where:
d – Deformation of teeth at pitch line under applied load W, in
E_1, E_2 – modulus of elasticity of material, psi
F – Face width, in
W – Tangential applied load, lbf

For spur steel gears with a modulus of elasticity of 207 GPa (30 x 10^6 psi) equation 9 simplifies to the following.

$$d = \frac{W/F}{1.667 \times 10^6} \quad (10)$$

The stiffness per unit of face width in the tangential direction would then be calculated per equation 11.

$$K^* = \frac{W/F}{d} = 1.667 \times 10^6\ lbf/in/in \quad (11)$$

With helical gears the deflection in the plane of rotation will be greater than in the direction normal to the teeth. Buckingham gives the equation 12 for the deflection in the plane of rotation for helical gears.

$$d = \frac{d_n}{\cos^2(\psi)} \quad (12)$$

Where:
d – Deformation of teeth at pitch line in the plane of rotation, in
d_n – Deformation of the teeth at the pitch line in the normal plane (d for a spur gear), in
ψ – Helix angle, degrees

Where the deflection and stiffness per unit of face width becomes equation 13 and 14 respectively.

$$d = \frac{9.000\frac{W}{F}\left(\frac{1}{E_1}+\frac{1}{E_2}\right)}{\cos^2(\psi)} \quad (13)$$

$$K^* = \frac{W/F}{d} = \frac{\cos^2(\psi)}{9.000\left(\frac{1}{E_1}+\frac{1}{E_2}\right)} \quad (14)$$

For steel helical gears the stiffness per unit face width can be calculated with equation 15.

$$K^* = \frac{W/F}{d} = 1.667 \times 10^6 \cos^2(\psi)\ lbf/in/in \quad (15)$$

Therefore the helical gear mesh stiffness can be determined by equation 16.

$$K = \frac{W}{d} = F\ 1.667 \times 10^6 \cos^2(\psi)\ lbf/in \quad (16)$$

The formula given by equation 16 is essentially the same as the K' formula given in API 684, equation 4, but the C constant is 1.667 rather than 1.75. This stiffness constant is dependent on tooth form and gear geometry and there are several published values or calculation methods that can be used to estimate the mesh stiffness.

AGMA 2001 suggests mesh stiffness constant values anywhere from 1.5 to 3 lbf/in/uin. Dudley [1984] states stiffness constant for mesh deflection are not known with certainty but based on testing stiffness values of 20 - 25 N/mm/um are reasonable for 20 degree pressure angle gears with low helix angles.

ISO 6636-1 details methods to determine single tooth stiffness and mesh stiffness, but states for steel gears with basic rack profile meeting ISO 53 and a few other common parameters a single tooth stiffness of 14 N/mm/um and a mesh stiffness of 20 N/mm/um can be used.

The published values of stiffness are in the base tangent plane. To be useful in rotordynamic codes the mesh stiffness is transformed from the base tangent direction into x and y Cartesian coordinates in the following equations, see Figure 11.

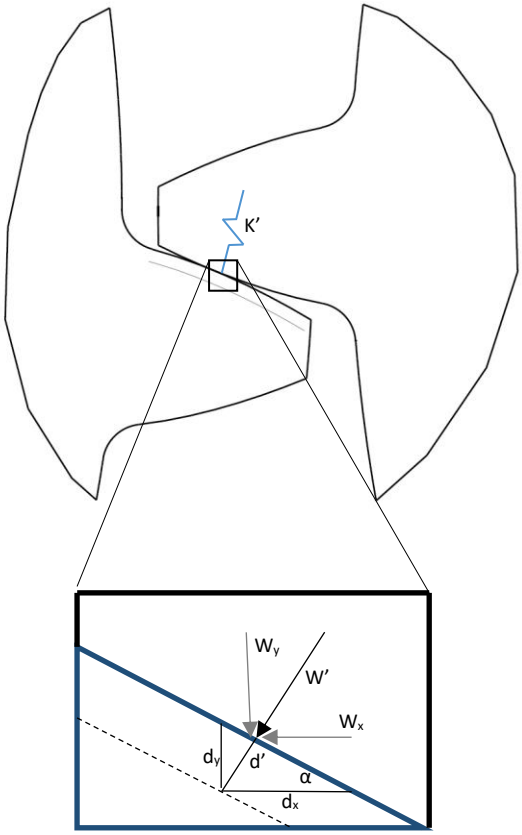

Figure 11. Gear tooth contact and planes of action.

$$K' = \frac{W'}{d'} \quad (17)$$

$$\begin{bmatrix} K_{xx} & K_{xy} \\ K_{yx} & K_{yy} \end{bmatrix} = \begin{bmatrix} \frac{W_x}{d_x} & \frac{W_x}{d_y} \\ \frac{W_y}{d_x} & \frac{W_y}{d_y} \end{bmatrix} \quad (18)$$

$$W_x = W' \sin(\alpha) \quad (19)$$

$$W_y = W' \cos(\alpha) \quad (20)$$

$$d_x = \frac{d'}{\sin(\alpha)} \quad (21)$$

$$d_y = \frac{d'}{\cos(\alpha)} \quad (22)$$

Where:
K' – Stiffness in base tangent plane, N/m
K_{xx} – Direct stiffness in x direction, N/m
K_{yy} – Direct stiffness in y direction, N/m
K_{xy} – Cross coupled stiffness relates force in x and displacement in y, N/m
K_{yx} – Cross couples stiffness relates force in y and displacement in x, N/m

W – Gear force N
d – Gear tooth displacement, m
α – Pressure angle, degrees
Directional subscitps:
‘ – Base tangent direction
x – X coordinate direction
y – Y coordinate direction

Substituting equation 19 through 21 into equation 18 gives equation 23.

$$\begin{bmatrix} K_{xx} & K_{xy} \\ K_{yx} & K_{yy} \end{bmatrix} = \begin{bmatrix} K'\sin^2(\alpha) & K'\sin(\alpha)\cos(\alpha) \\ K'\sin(\alpha)\cos(\alpha) & K'\cos^2(\alpha) \end{bmatrix} \tag{23}$$

Equation 23 is equivalent to the API 684 equations 5 through 8. The API calculations add some adjustments to provide the proper sign for the coefficients based on the loading and rotation. The angle γ used in the API equations is a complementary angle of α so sin(α)=cos(γ).

For simplification these derivations assume that the pressure angle in the normal plane to the gear teeth and in the tangential or rotational plane are near the same and the helix angle at the pitch line to be near the same to the helix angle at the base diameter. For an order of magnitude estimate of the mesh stiffness the assumptions are sufficient for rotordynamic analytics and simplify the equations significantly.

Thrust Collar Dynamic Coefficients

Thrust collars are frequently applied in integrally geared turbomachinery, using a single helical gear, to transmit axial loads from the compressor/expander stages directly to bull gear main disk. The area of the load transmission is relatively small as it is formed by overlapping sections of the outer diameters from the bull gear and a thrust collar on the pinion gear. A hydrodynamic oil film is established to keep the bull gear face separate from the pinion thrust collar. San Andres, et. al. [2014] shows the approach to thermal-mechanical and dynamic assessment of thrust collars to understand their performance characteristics. A thrust collar relies on similar hydrodynamic principles as a thrust bearing. The difference being that relative motion between the bull gear face and the thrust collar face must be considered as both surfaces are in rotation around different axes, illustrated in Figure 12.

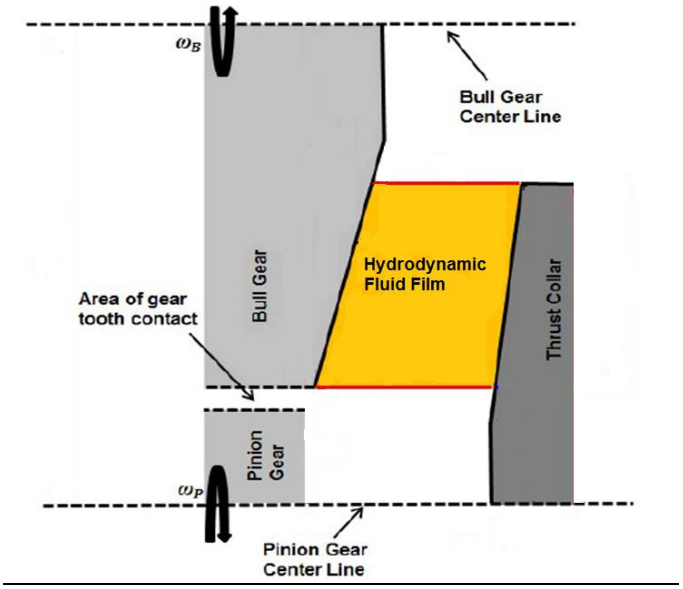

Figure 12. Hydrodynamic Function of Oil Lubricated Thrust Collar

Cable, T., et. al. [2016], show that the hydrodynamic oil film that is established generates an axial stiffness and damping, as shown in Figures 13 and 14. These dynamic coefficients act to couple the dynamics of the bull gear and pinion axial motion. Variations in the alignment between the pinion thrust collar face and the bull gear face changes the hydrodynamic film and shifts the dynamic characteristics.

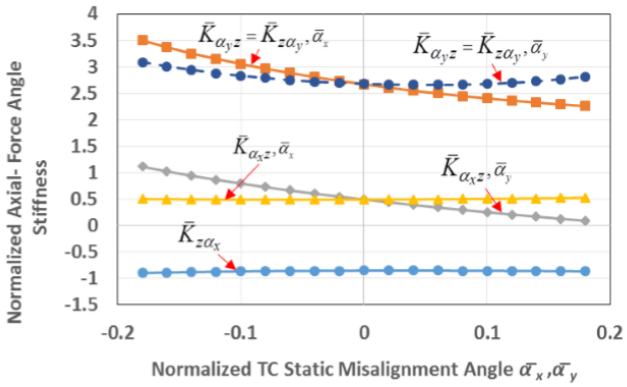

Figure 13. Influence of alignment on the axial stiffness that couples bull gear and pinion dynamics. (Ref. Cable et. al, 2016)

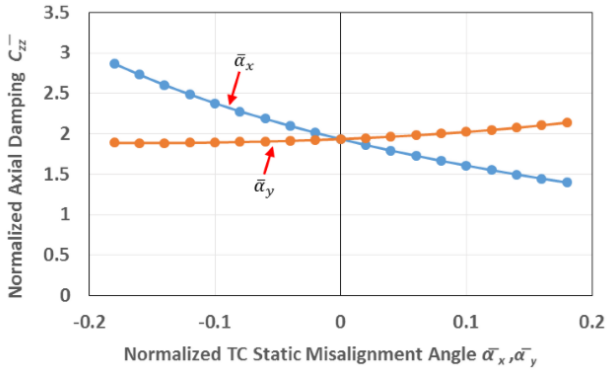

Figure 14. Influence of alignment on the axial damping that couples bull gear and pinion dynamics. (Ref. Cable et. al, 2016)

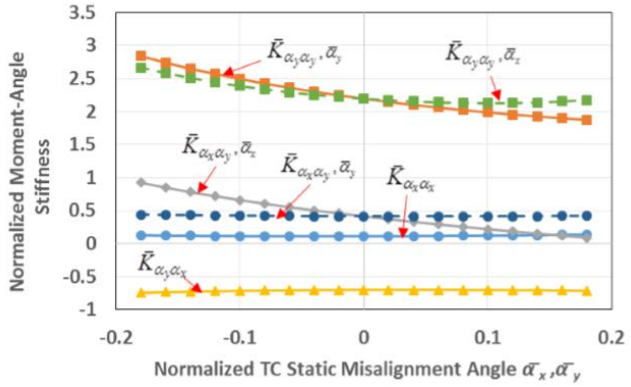

Figure 15. Influence of alignment on the moment angle stiffness that couples bull gear and pinion dynamics. (Ref. Cable et. al, 2016)

In addition to the axial dynamic coefficients, additional dynamic coefficients are also generated by the hydrodynamic oil film in reaction to perturbations in the alignment conditions. Dynamic moment coefficients are produced that couple the lateral motion of the bull gear and the pinions. Figures 15 shows how variations in the alignment may affect the moment angle stiffness. The most important consideration is that there is a coupling present between the bull gear motion and the pinion motion. Typically the inertia of the bull gear is order of magnitude greater than that of the pinion meaning that bull gear motion is more apt to be imparted on the pinion than the other way around.

ROTORDYNAMIC ANALYSES

Background

An accurate rotordynamic analysis is key to developing a mechanically robust compressor design. Lateral assessment of pinions and bull gear rotors is typically conducted in isolation of each other. Most pinions operate between the second damped peak response speed and the third damped peak response speed. The ratio of the pinion speed to the damped first critical speed can range from 8:1 to 1.1:1. For the higher pinion speed ratios the units may be highly susceptible to instabilities and substantial care/effort must be taken to minimize instability risk. Designing the pinion shafts requires iterating the unbalance response and stability characteristics of the pinion with mechanical design considerations such as: gear machining, gear box layout, gas path sealing etc. For the unbalance response other practical considerations come into play such as the required balancing approach. Schnieder [1987] gives an excellent overview of different classes of balancing depending upon shaft flexibility. Ultimately the designer tries to avoid the need for high-speed balancing as this complicates field repair but for high performance machines operating at high speeds this can become a requirement. Most IGCs only require low speed balancing due to the limited shaft length (only two stages per pinion.)

For the bull gear the primary factor influencing lateral rotordynamics is the coupling center of gravity and the half weight of the coupling. From the rotordynamics perspective the intent is usually to minimize the coupling weight/inertia and overhung center of gravity to the greatest extent possible.

Advanced analytics can be conducted to couple the bull gear and pinion lateral vibration. There are two coupling mechanisms between the bull gear and the pinions: mesh stiffness and thrust collar moment stiffness.

To demonstrate the influence of coupling from gear mesh stiffness and/or thrust collar moment stiffness a typical high-speed pinion case is examined. Even though the case chosen had 3 pinions in actuality only one pinion and the bull gear is analyzed to demonstrate the concepts. The basic geometry of the rotor-bearing-gear system is given in Tables 1 through 4.

Table 1. Pinion and bull gear shaft geometry and material properties.

Parameter	Pinion	Bull Gear
Shaft Material	*AISI 4140*	*AISI 4140*
Disk Materials	*Ti6Al4V*	*AISI4140*
Type of Impeller	*Closed*	*n.a.*

Table 2. Bearing geometry.

Parameter	Pinion Shaft	Bull Gear Shaft
Type	*TPJB*	*3 Axial Groove*
Diameter	*50*	*120*
Length	*30*	*85*

Table 3. Gear geometry.

Parameter	*Pinion Shaft*	*Bull Gear Shaft*
Rotational Speed (rpm)	*28,527*	*3552*
Design Power (kW)	*3,170*	*3,216*
Helix Angle (deg)	*15*	*15*
Pitch Diameter(mm)	*99.654*	*807.65*
Face Width (mm)	*84*	*80*

Table 4. Thrust collar geometry.

Parameter	*Pinion Shaft*	*Bull Gear Shaft*
Thrust Collar OD (mm)	*150*	*788*
Distance Between Centers (mm)	*451*	
Contact Angle (deg)	*1*	

Independent Shaft Lateral Rotordynamic Analyses

A critical speed map is created for the uncoupled pinion and bull gear of the example case chosen. The critical speed map (Figures 16 and 17) shows how the undamped critical speeds vary as a function of the bearing (or support) stiffness applied to the rotor. The lowest two modes (rigid rotor modes) begin at near zero Hertz and move upwards in frequency until sufficient stiffness is present to pin the bearing/support locations. Flexible shaft modes begin at a free-free frequency and also increase in frequency until the bearings positions become pinned as nodes. Also plotted on the map are the projected bearing stiffness. Where these lines cross the undamped natural frequencies is the approximate location of critical speed of the shafts for a lightly damped shaft.

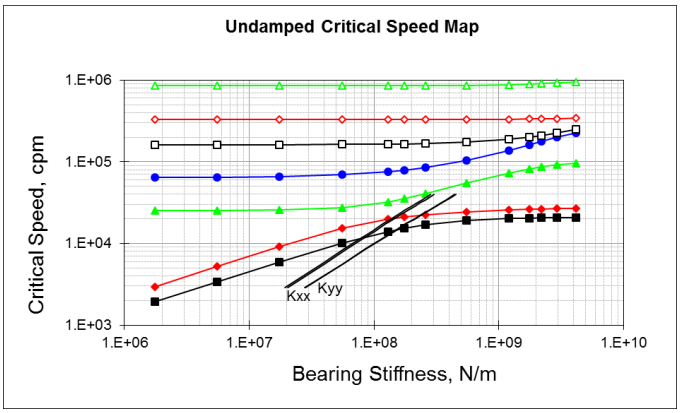

Figure 16. Undamped Critical Speed Map of Pinion Shaft

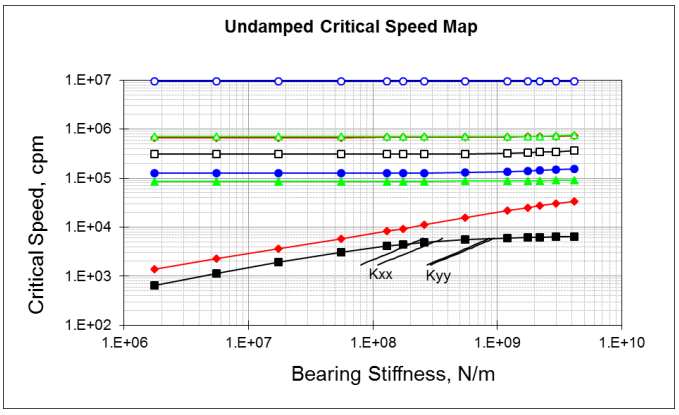

Figure 17. Undamped Critical Speed Map of Bull Gear Shaft

To examine the sensitivity of the turbomachinery to imbalance forced response, unbalance response analyses are conducted. The forcing function applied most commonly is a synchronous excitation of the shafts from unbalance. The key aspects for consideration are proximity (separation margin) to peak response speeds. And how well damped (amplification factor) the peak responses speed are. Figures 18-20 show the unbalance response (bode plots) of the pinion shaft and bull gear shaft at critical location and as a result of different unbalance excitation zones. A diagram of how the unbalance is applied can be seen inset on the figures, with the in plane unbalance with both unbalances in the same orientation with respect to the plane of rotation and the out of plane unbalance has the unbalances on opposite sides of the shaft with respect to the plane of rotation.

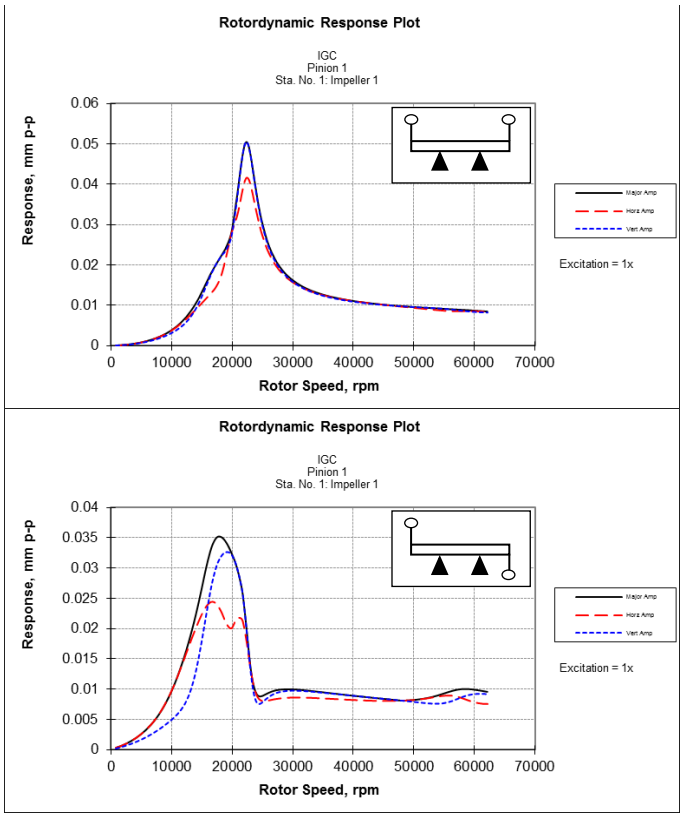

Figure 18. Bode Plot of Stage 1 End of Pinion Shaft with In Plane and Out-Plane Unbalance

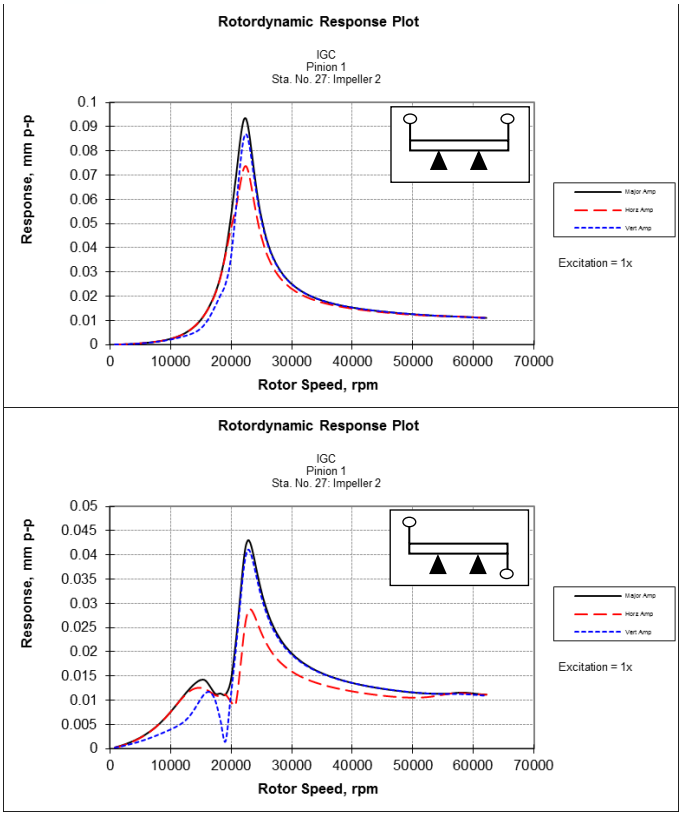

Figure 19. Bode Plot of Stage 2 End of Pinion Shaft with In Plane and Out-Plane Unbalance

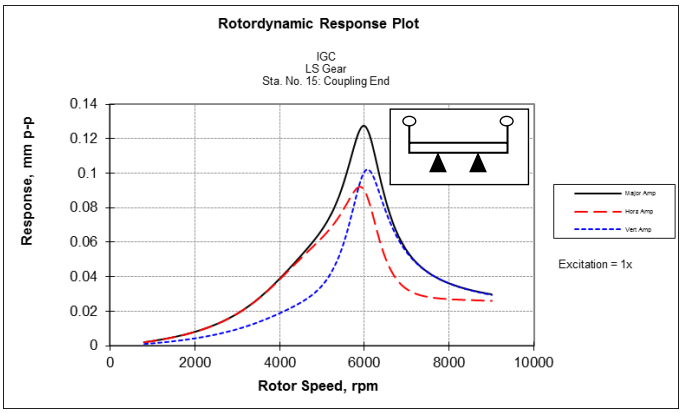

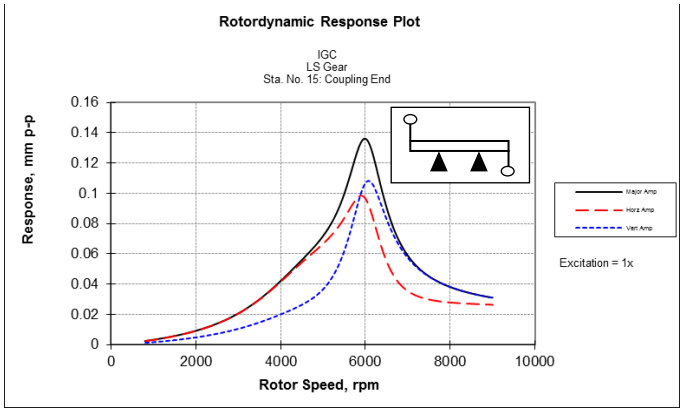

Figure 20. Bode Plot of Coupling End of Bull gear shaft with In Plane and Out-Plane Unbalance

The shapes of the modes being excited by the unbalance provide insight into critical areas of motion and excitation. These mode shapes also can be used to provide some understanding how the coupling of the bull gear and the pinions may influence the dynamics. Figure 21 shows the damped mode shapes. Coupling between the pinion shaft and the bull gear shaft occurs at the center of the gull gear and pinion gears. If no motion is present at the bull gear or pinion shaft coupling locations then the modes will remain independent. If substantial motion is present at both the coupling locations then the potential for strong dynamic coupling exists.

Establishing sufficient separation margin for critical speeds is critical to integrally geared machinery. Variations in the axial load changes the direction and magnitude of the bearing loads and thereby shifts dynamic coefficients and also influences the level of moment stiffness from the thrust collars (if present.) Also as the compressor loading shifts this alters the gear forces and the bearing reactions. Therefore it is critical to assess a number of variables when establishing separation margins for the critical speeds.

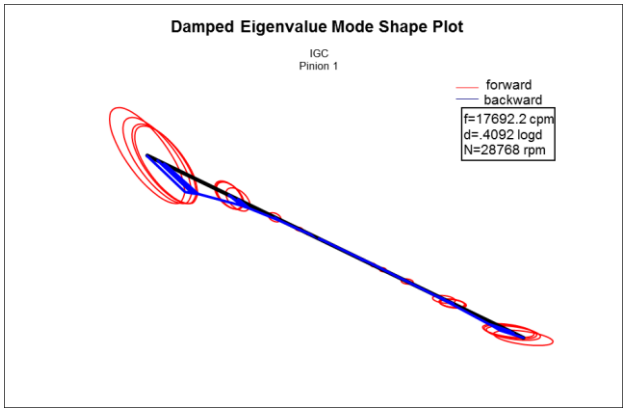

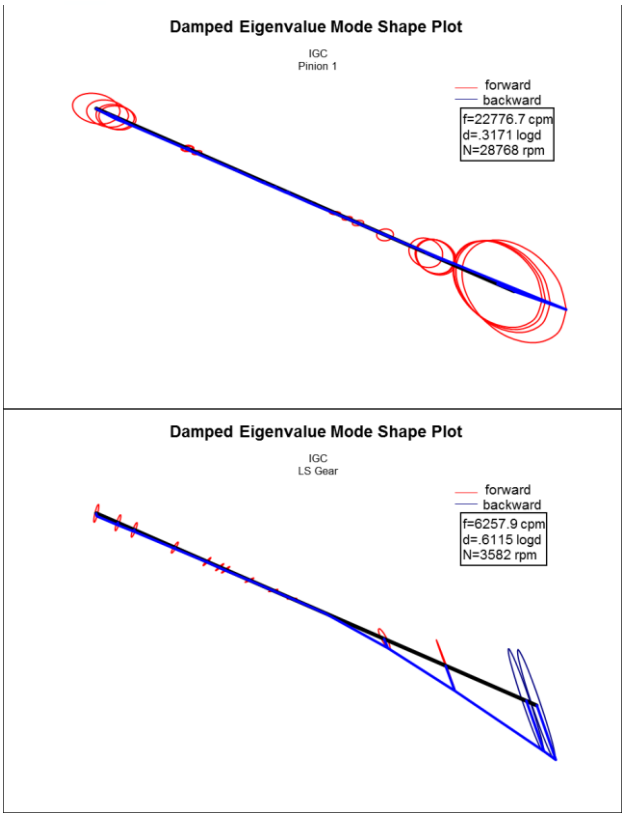

Figure 21. Operating Speed Deflected Mode Shapes with In Plane and Out-Plane Unbalance

Coupled Bull Gear and Pinion Lateral Analyses

The gear mesh stiffness and the thrust collar moment stiffness couples the bull gear and pinion dynamics. Figure 22 - 25 show the impact of coupling the bull gear and pinion dynamics. As the torque level increases the amount of gear mesh stiffness increase proportionally. The peak response speeds shift a negligible amount. And the amplification factor changes negligibly, however there is a small increase in the amplitude of vibration. As the axial load increases the amount of moment stiffness from the thrust collar increases proportionally, which would increase the coupling.

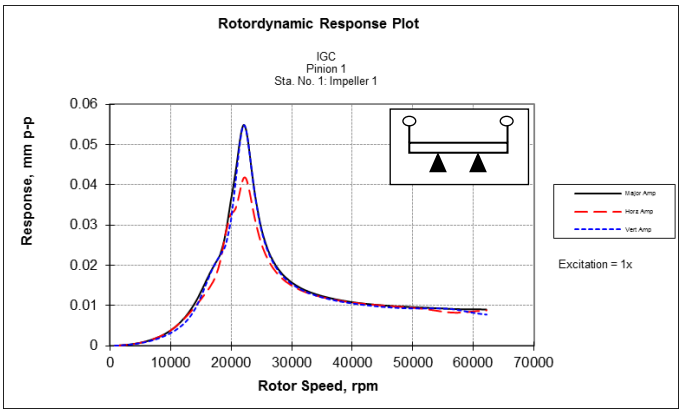

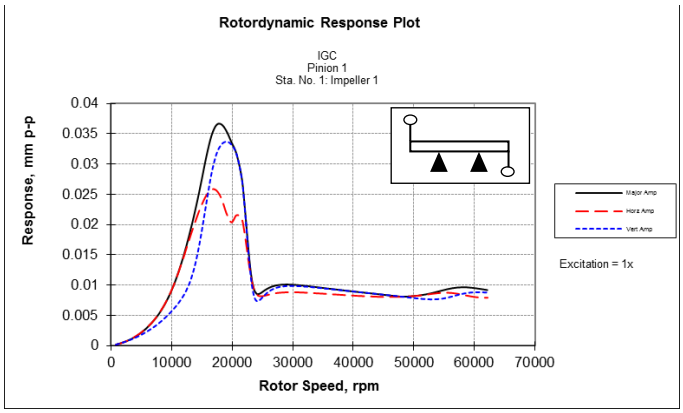

Figure 22. Bode Plot of Stage 1 End of Pinion Shaft with In Plane and Out-Plane Unbalance

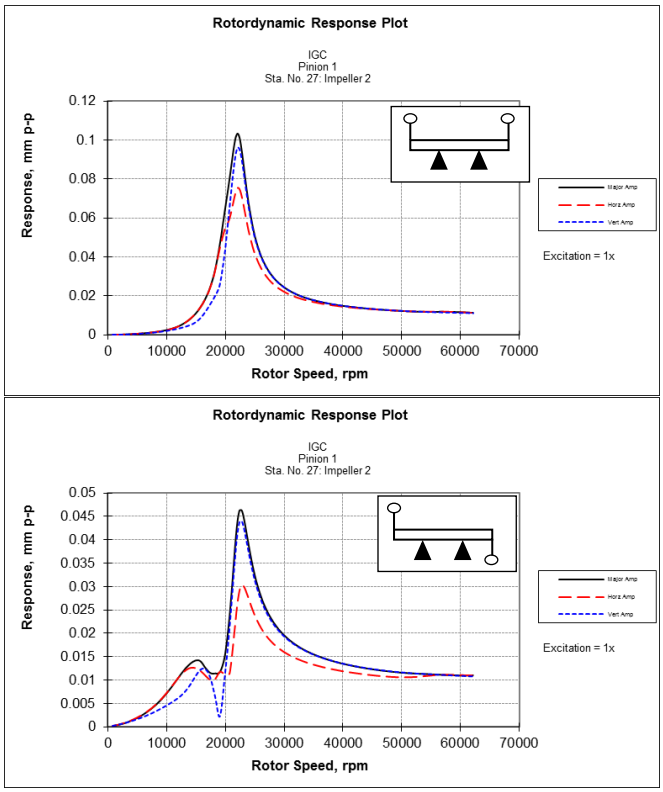

Figure 23. Bode Plot of Stage 2 End of Pinion Shaft Figure with In Plane and Out-Plane Unbalance

The influence of the bull gear on the dynamics of the pinion depends on two factors: 1. the level of stiffness in the gear mesh and the moment stiffness of the thrust collar and 2. That pinion motion to be present at the pinion interface with gear location. The lower two mode shapes are typically overhang mode shapes with minimal motion present at the pinion gear location.

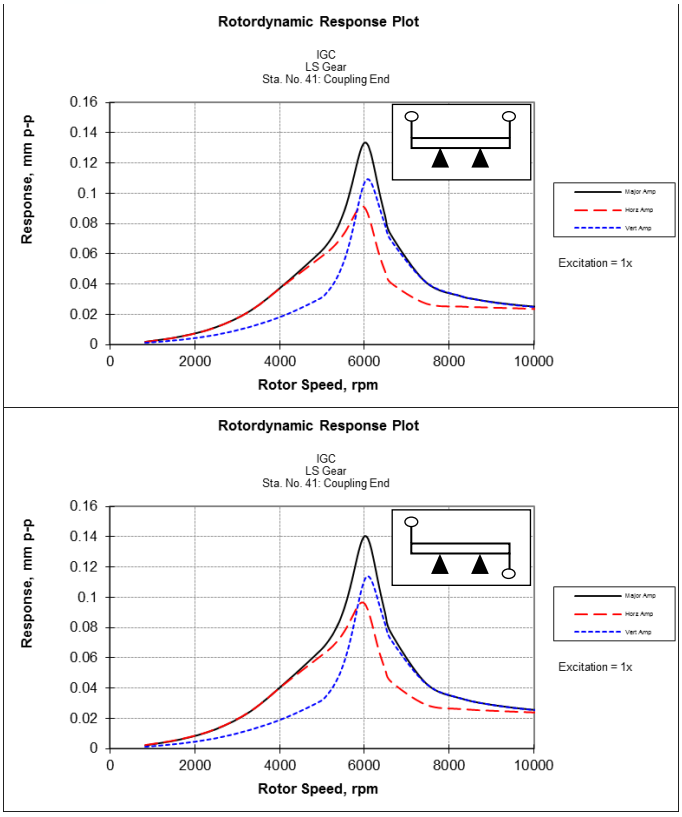

Figure 24. Bode Plot of Coupling End of Bull gear shaft with In Plane and Out-Plane Unbalance

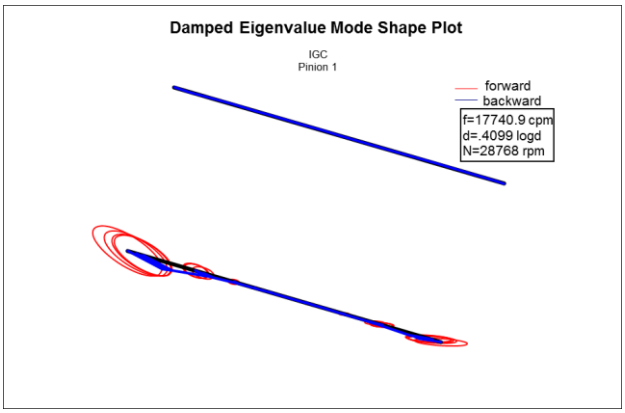

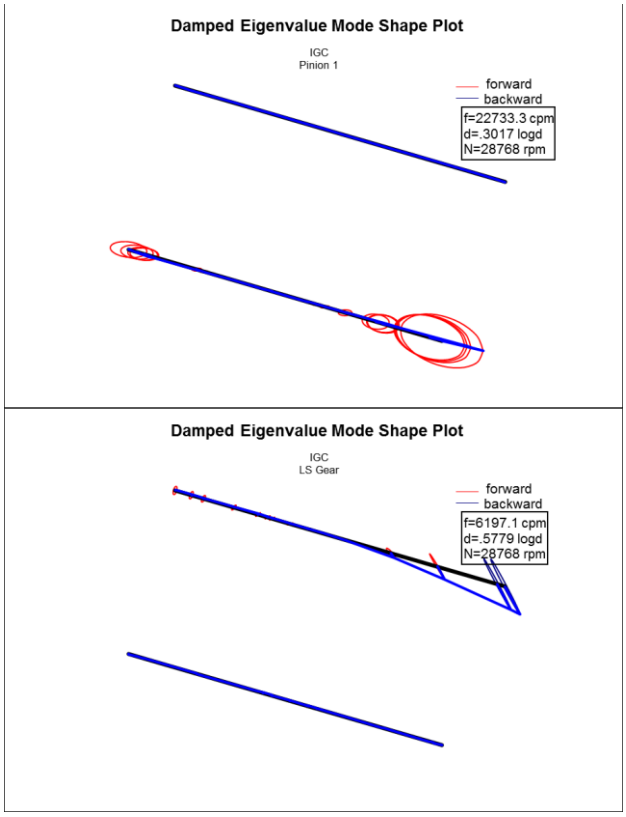

Figure 25. Operating Speed Deflected Mode Shapes with In Plane and Out-Plane Unbalance

Lateral Instability of Pinion Shafts

Turbomachinery can develop instabilities that are related to the shaft, bearings, seals, and/or aerodynamics of the compressor or expander. To assess the risk from developing an instability a lateral eigenvalue analysis is conducted. The key eigenvalues that may become unstable in turbomachinery are the lower order forward whirl modes. The largest unknown in a machine is the level of aerodynamic cross-coupling, which may drive the instability. Stability plots can be generated that show the resulting log decrement of modes as function of aerodynamic cross-coupling. Figure 26 plots the log decrements of the three lowest forward whirl modes against aero-dynamic cross-coupling. The plot shows the predicted variation when considering and omitting coupling to the bull gear shaft. Notice that the coupling results in a slight reduction of the log decrement of the first and second forward whirl modes. The log decrement of the third mode is substantially reduced, but insensitive to aerodynamic cross-coupling.

To examine the influence of the critical speed ratio on the stability margin the mass of the overhang impellers was increased (the original impellers were titanium, the plot illustrates the influence of shifting to a more dense material or larger diameter impeller.) Figure 27 shows a plot of how the undamped critical speed ratio influence the stability margin. Notice that the trend remains constant for the coupling of bull

gear and pinion to reduce stability margin.

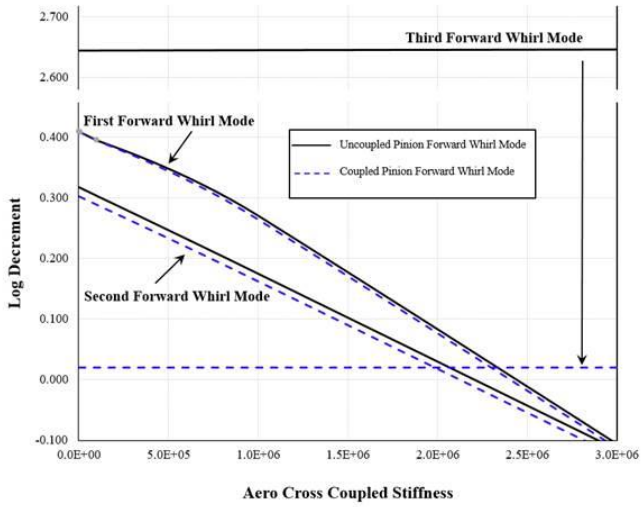

Figure 26. Instability Map of Coupled and Uncoupled Bull and Pinion Gears.

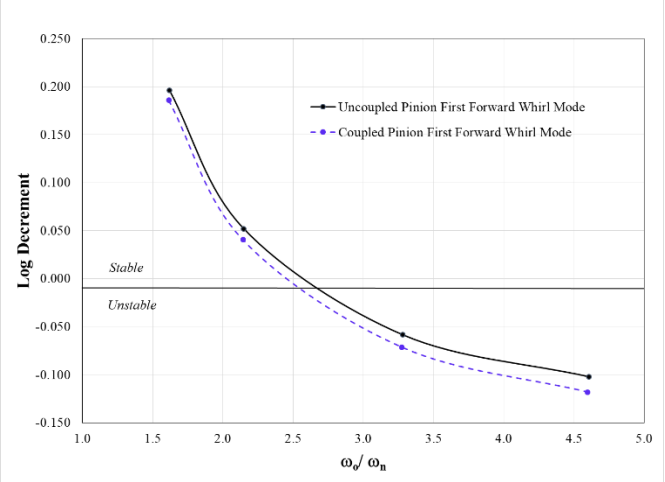

Figure 27. Influence of Critical Speed Ratio on Stability Margin.

Sub-Synchronous Excitation of Pinion Shafts

With the ability to couple the bull gear and pinion shafts it now becomes possible to examine the impact of synchronous bull gear shaft excitations on the reaction of the pinion. As the pinion shaft rotation increases the synchronous bull gear shaft excitation shows as a sub-synchronous pinion vibration. As the pinion shafts of integrally geared turbomachines frequently operate at multiples of critical speeds the resonance conditions of the pinion can be excited by the bull gear. Figure 28 shows the pinion shaft response as a result of simultaneous synchronous excitations of bull gear and pinion. The figure shows just the operating speed of the pinion, with the lower frequency excitation from the bull gear unbalance. The amount of pinion motion depends upon the coupling level and the proximity of the pinion response to the bull gear excitation frequency.

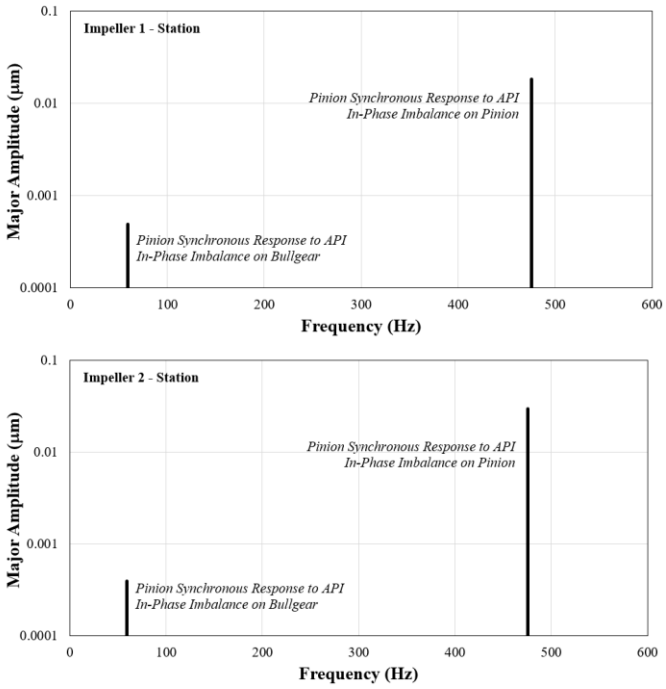

Figure 28. Synchronous Excitation of Bull Gear and Pinion Super-Imposed at Running Speeds

The lateral and axial motions of the bull gear are coupled when a thrust collar is present. The angled face of the thrust collar allows for motion in the axial, or lateral, plane to be transferred to the corresponding plane. Although this author is not aware of any instances where excessive vibration has resulted from this coupling it is worth considering that misalignment of the bull and pinion gear faces can translate into harmonic excitations of the pinion shaft Childs, et. al. [2017.]

COMMON VIBRATION CHARACTERISTIICS

General Sources of Vibration

An integrally geared turbomachine is susceptible to the same type of excitations as any turbomachine. These common turbomachinery vibrations divide into two categories: forced and self-excited. The forced vibrations emanate most frequently from excessive unbalance, insufficient separation from resonances, and/or poor damping characteristics. This author also includes misalignment as potential source of forced vibration. The self-excited vibrations, instabilities, are related to large aerodynamic excitations, large levels of cross-coupling, and/or insufficient stability margin. Integrally geared machines are also prone to additional types of forced vibration: excitations from other coupled shafts and/or meshing related issues. Table 5 gives the common signatures of unwanted vibration characteristics for integrally geared turbomachines. A challenge in diagnosing the root cause of vibration is that different root

causes may have the same signature, or a root cause may have different signatures due to variations in the individual machine.

Table 5. Common vibration characteristics associated with integrally geared turbomachinery.

Potential Origin	Bull Gear Vibration	Pinion Vibration
Pinion resonance near bull gear excitation	*n.a.*	*1 x f_{bg}*
Loose thrust collar	*n.a.*	*1x, 2x, 3x, and 4x f_{bg}*
Flow field excitation from pipe turning	*n.a.*	*Broad band sub-synchronous*
Spherical pivot tpjb "stiction"	*n.a.*	*Broad band sub-synchronous*
High pinion unbalance	*n.a.*	*1 x f_p*
High bull gear unbalance	*1 x f_{bg}*	*n.a.*
Pinion Shaft instability	*n.a.*	*ω_n*
Insufficient SM from Pinion Resonance	*n.a.*	*1 x f_p*
Morton Effect	*n.a.*	*Cyclic variation of f_p over time.*
Pinion Journal Bearing Oil Starvation	*n.a.*	*Broad band sub-synchronous*

Three specific examples are presented of vibration related issues that are specific to integrally geared turbomachines.

Bull Gear Harmonics Transposed on Pinion Vibration

Bull gear harmonics are frequently present on pinion shafts. These vibration patterns are not the result of rotor-bearing instabilities, despite having a sub-synchronous characteristic. Instead these patterns of vibration are forced vibrations with amplitude that vary as a result of: 1) magnitude of lateral vibration present in the bull gear, 2) sensitivity of the pinion shaft to excitations from the bull gear, and/or 3) interaction from misalignment of the thrust collar to the bull gear face. If the amplitude of vibration is low relative to the overall vibration spectrum that is not point of concern. If the vibration levels are elevated then the root cause needs to be determined and corrective action taken. Root cause determination requires examining: 1) bull gear shaft synchronous vibration levels (particularly at bull gear) 2) pinion bode plot and mode shapes to examine sensitivity at or near bull gear excitation frequencies, 3) alignment records. Figure 29 shows a typical vibration characteristic of a pinion highlighting relevant frequencies. Note this is typical and not a cause for concern. It is only when the vibration levels exceed API guidelines that a concern is present,

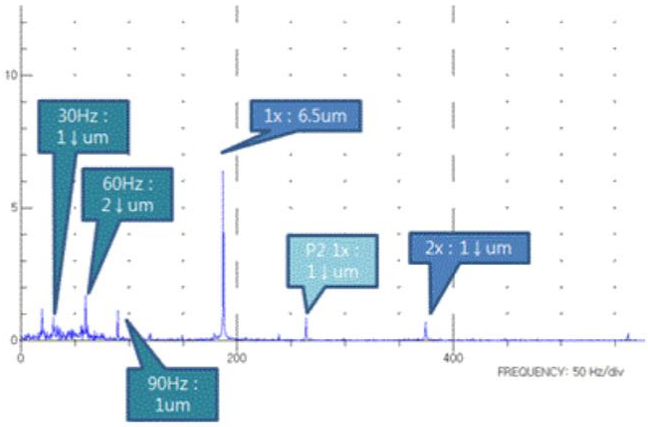

Figure 29. FFT of a typical pinion vibration levels.

Gear Induced Vibration

One key indicator of a serious vibration issue that requires immediate attention is step increases in vibration amplitude that is not related to changing operating conditions. In this particular example the synchronous vibration was increasing in step increments over a period of several months. Even though the vibration level was below alarm or trip levels the best approach is to determine the root cause at the earliest possible time. The point of concern is that step increases are related to sudden changes in balance condition. These step changes in balance condition can be related to: component in the rotating assembly slipping, ingestion of foreign material, and/or fracture(s) propagating. All of which can lead to substantial and catastrophic damage if left untreated. Figure 30 shows the amplitude of vibration over time. Notice the highlighted areas. The unit was shut down and inspected and fractured pinion teeth were discovered. Figure 31 shows the fractured tooth. Additional teeth were also showing signs of fracture propagation. The root cause was related to gear tooth scuffing and corrected by improved surface finish and slight modification of the tooth profile.

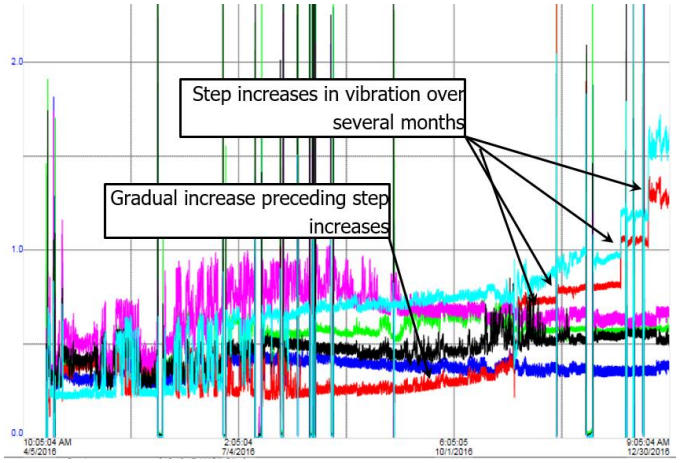

Figure 30. Vibration Amplitude Tracked Over Several Months of Operation (Spikes are Start-up and Shut-downs)

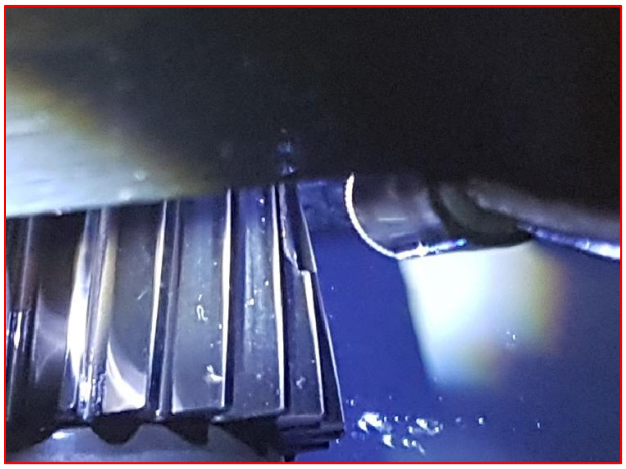

Figure 31. Fractured Pinion Tooth

Oil Starvation Due to Windage

In high-performance bearings it is possible to apply directed lubrication to the bearings in order to decrease the level of hot-oil carry over from one tilting pad to the next pad. To further reduce the hot oil carry over open end seals can be applied. However, in geared systems the presence of the gear wheels creates substantial windage that can act to pull oil from the pad and cause starvation. Figure 32 shows the vibration pattern resulting from such starvation. The plots shows the vibration frequency spectrum resulting from a Fast Fourier Transform (FFT) of proximity probes on opposing ends of the pinion shaft. The corrective action is to apply a shield, or end seal on the bearing closest to the gear. When such shield is applied the oil starvation from windage is improved and the vibration levels reduced. Figure 33 shows the vibration pattern of the same machine once a windage shield is applied, notice how the sub-synchronous vibration, once dominating and wide is all but eliminated.

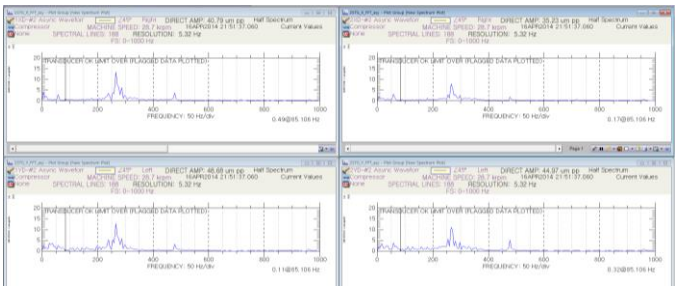

Figure 32. FFT of Pinion of Proximity Probes with Directed Flow TPJB and No End Shield

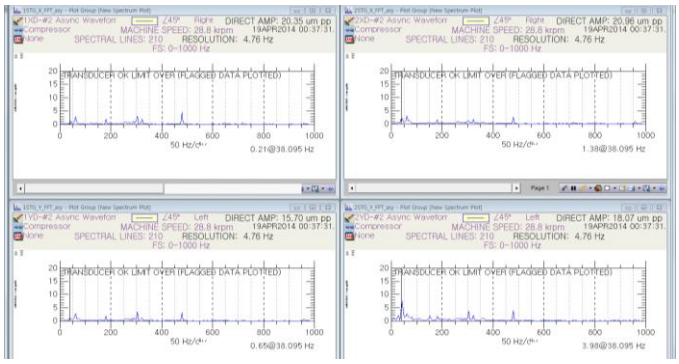

Figure 33. FFT of Pinion of Proximity Probes with Directed Flow TPJB and End Shield Applied on Gear Side

CONCLUSIONS

Several aspects related to the rotordynamics of integrally geared systems are discussed:

1. The type of thrust mechanism applied on the pinion has an influence on the neat radial loads in the bearings.
2. Thrust collars and gear interaction couple the dynamics of the bull and pinion gear system. However, for integrally geared machines that level of coupling is typically minimal.
3. The reason that the coupling is minimal is that the mode shapes for the pinions first and second modes place the gear near a node.
4. The vibration characteristics of typical operation of gear systems and typical issues is reviewed.
5. Variations in the compressor loading will shift the critical speeds and therefore considerable care must be given to establishing sufficient separation margin.

NOMENCLATURE

Variables

A	= 1 for downloaded rotors and = -1 for uploaded rotors	
B	= 90° for clockwise rotation = 270° for counter clockwise rotation	
C	= 12.057 for metric = 1.75 English units	
d	= Gear tooth displacement	(m)
E_1, E_2	= Modulus of elasticity of material	(psi)
FW	= Effective Face Width	(mm,in)
K	= Stiffness	(N/m, lbf/in)
K*	= Stiffness per unit face width	(N/nm/μm, lbf/in/μin)
W	= Gear force	(N)
α	= Normal Pressure Angle	(degrees)

β	= Helix Angle	(degrees)
γ	= (Aα)+B	
ω	= Frequency	(Hz)

Subscripts

xx	= Direct stiffness in x direction
yy	= Direct stiffness in y direction
xy	= Cross coupled stiffness relates force in x and displacement in y, N/m
yx	= Cross couples stiffness relates force in y and displacement in x, N/m
n	= First Natural Frequency
o	= Operating (Rotational) Frequency
p	= Pinion
bg	= Bullgear

REFERENCES

AGMA 925-A03, Effect of Lubrication on Gear Surface Distress, American Gear Manufacturers Association 500 Montgomery Street, Suite 350, Alexandria, Virginia 22314.

AGMA Standard 2001-D04 Fundamental Rating Factors and Calculation Methods for Involute Spur and Helical Gear Teeth, American Gear Manufacturers Association 500 Montgomery Street, Suite 350, Alexandria, Virginia 22314.

AGMA Standard 2101-D04 Fundamental Rating Factors and Calculation Methods for Involute Spur and Helical Gear Teeth, American Gear Manufacturers Association 500 Montgomery Street, Suite 350, Alexandria, Virginia 22314.

AGMA Standard 6011 Specification for High Speed Helical Gear Units, American Gear Manufacturers Association 500 Montgomery Street, Suite 350, Alexandria, Virginia 22314.

API Standard 613 Special Purpose Gear Units for Petroleum, Chemical, and Gas Industry Service Fifth Edition, American Petroleum Institute, Washington, D.C., 2007.

API Standard 617 Axial and Centrifugal Compressors and Expander-compressors for Petroleum, Chemical and Gas Industry Services, Seventh Edition American Petroleum Institute, Washington, D.C., 2009.

API Standard 671 Coupling Standard, Fourth Edition American Petroleum Institute, Washington, D.C., 2007.

API Standard 672 Packaged, Integrally Geared Centrifugal Air Compressors for Petroleum, Chemical, and Gas Industry Services, Fourth Edition, American Petroleum Institute, Washington, D.C., 2004.

API Standard 684 Rotordynamic Tutorial: Lateral Critical Seepds, Unbalance Response, Stability, Train Torsionals, and Rotor Balancing, Second Edition American Petroleum Institute, Washington, D.C., 2005.

Beaty, P.J., Eisele, K., and Schwarz, C. "Integrally Geared API 617 Process Gas Compressors," Proceedings of the Twenty-Ninth Turbomachinery Symposium, 2000.

Buckingham, E., "Analytical mechanics of gears," Dover Publications, New York, 1949

Cable, T. A., San Andres, L., Wygant, K. "On the Predicted Effect of Angular Misalignment on the Performance of Oil Lubricated Thrust Collars in Integrally Geared Compressor," Proceedings of the 61st ASME Turbo Expo ASME IGTI 2016.

Childs, D., and Crandall, A., "A Simple (1-Flexible Rotor) Model That Shows Bull Gear Runout as a Source of Sub-synchronous, Lateral, Vibration in Integrally Geared Compressor (IGC) Pinions" Turbo Expo 2018 GT2018-75326

Dudley, D.W. "Practical gear design," McGraw-Hill, Inc. 1984

Fingerhut, U., Rothstein, E. Strez, G. "Standardized Integrally Geared Turbomachines – Tailor Made For the Process Industry," Proceedings of the Twenty-Ninth Turbomachinery Symposium, 1991.

Gruntfest, P.M., Andonis, L., and Marscher, W.D. "Rotor Instability Problems in an Integrally Geared Compressor Supported by Tilting Pad Bearings," Proceedings of the Twenty-Ninth Turbomachinery Symposium, 2001.

ISO 6336-1 Calculation of load capacity of spur and helical gears, "Part 1: Basic principles, introduction and general influence factors," International Organization for Standardization, Case Postale 56, CH-1211 Geneve 20, Switzerland, 1996

San Andres L., Cable, T., and Wygant, K. "On the Predicted Performance of Oil Lubricated Thrust Collars in Integrally Geared Compressors," ASME GT2014-25914, 2014.

Smith, P. "Crosstalk Vibration in an Integrally Geared Turbocompressor," Energy-Tech.com, August 2011

Srinivasan, A. and Impasto, C. "Application of Integrally Geared Compressors in the Process Gas Industry," GT2013-95870, Proceedings of ASME Turbo Expo, 2013.

Srinivasan, A., "Differentiating Benign and Unstable Vibrations in Integrally Geared Centrifugal Compressors," ASME Turbo Expo, Copenhagan Denmark, Paper No. GT2012-

69071.

Wehrman, J. G., Walder, T. E., Haryett, N. J. "The Use of Integrally Geared Compressors Based on Two Industrial Gas Companies' Experience," Proceedings of the Thirty-Second Turbomachinery Symposium, 2003.

Williams, E. A and Badini, J,R. "Causes of Subsynchonous Vibration in Integrally Geared Compressor," Proceedings of the 44th Turbomachinery & 31st Pump Symposium, 2015

Wygant, K. D. Bygrave, J., Bosen, W. Pelton, R. "Tutorial on the Application and Design of Integrally Geared Compressors," Asia Turbomachinery &Pump Symposium, 2016.

Zhang, M. Jiang, Z., Gao, J, "Dynamic Analysis of Integrally Geared Compressors with Vary Workloads," Hindawi Publishing Corporation Shock and Vibration Volume 2016.

ACKNOWLEDGEMENTS

The authors would like to extend their appreciation to Hanwha Power Systems for support of this publication.